Journal of Petroleum Research and Studies

journal homepage: https://jprs.gov.iq/index.php/jprs/

Print ISSN 2220-5381, Online ISSN 2710-1096

Corrosion Monitoring and Chemical Control in the Overhead System of Atmospheric Distillation Columns

Mahmoud Alhreez[1*], Aliaa S. Abd Al-ameer[2], Zolfa Q. Atshan[1], Xin Xiao[3]

[1]South Refineries Company, Thi-Qar Refinery, Ministry of Oil, Iraq.

[2]Department of Chemistry, College of Science, University of Thi-Qar, Iraq.

[3]College of Environmental Science and Engineering, Donghua University, Shanghai, China.

[*]Corresponding Author E-mail: mahmodeng22@gmail.com

Article Info

Received 01/06/2025
Revised 19/08/2025
Accepted 27/08/2025
Published 19/03/2026

DOI: http://doi.org/10.52716/jprs.v16i1.1141

Abstract

This study investigates corrosion in the overhead system of atmospheric distillation columns, focusing on the role of crude oil properties and chemical additives. Field observations, supported by laboratory analysis, revealed that elevated levels of BS&W, salts, and sulfur significantly contribute to corrosion, mainly due to acidic condensate formation and chloride-induced degradation. Corrosion rates varied with operating conditions and were confirmed by inspection of system components. Chemical treatment effectively mitigated corrosion when key process parameters such as pH and chloride concentrations were optimized. These findings highlight the importance of targeted chemical control to extend equipment life and ensure stable refinery operations.

Keywords: Overhead corrosion, Refinery overhead system, Corrosion mechanisms in refineries, Corrosion rate, Chloride-induced corrosion.

مراقبة التآكل والتحكم الكيميائي في منظومة الجزء العلوي لأبراج التقطير الجوي

الخلاصة

تهدف هذه الدراسة إلى تحليل سلوك التآكل في منظومة أعلى برج التقطير الجوي، مع التركيز على تأثير خصائص النفط الخام والمواد الكيميائية المضافة. أظهرت نتائج الرصد الميداني والتحليل المختبري أن ارتفاع نسب الرواسب والماء، والأملاح، والكبريت في النفط الخام يسهم بشكل كبير في التآكل من خلال تكوين مكونات حامضية وتفكك الطبقات السطحية بفعل الكلوريدات. تفاوتت معدلات التآكل تبعاً لظروف التشغيل، وتم تأكيد ذلك من خلال الفحص المباشر لأجزاء المنظومة

المتآكلة. أثبتت المعالجة الكيميائية فعاليتها في تقليل التآكل عند ضبط معايير التشغيل الفعالة مثل الرقم الهيدروجيني وتركيز الكلوريد. وتؤكد النتائج أهمية التحكم الدقيق في المعالجة الكيميائية لضمان استمرارية التشغيل وإطالة عمر المعدات في المصافي.

1. Introduction

Crude oil consists of a complex hydrocarbon matrix that contains impurities such as water, salts, solids, and trace metals. These impurities cause major operational issues in refinery units, specifically corrosion, fouling, and blockages, which reduce equipment lifespan and affect process performance [1]. Because of harsh conditions such as high temperatures, pH shifts, and the presence of metal ions, corrosion remains a persistent challenge in refining [2]. Frequent unit shutdowns for corrosion-related maintenance lead to significant maintenance costs, highlighting the need for focused inspection and preventive strategies [2-4].

The overhead system of atmospheric distillation columns is particularly vulnerable to corrosion due to elevated chloride levels [5]. It includes air-cooled exchangers (condensers), the overhead receiver (boot drum), reflux lines, and product withdrawal lines, where rising vapors condense and collect [6]. Hydrochloric acid (HCl) is a key corrosive species in this environment [7]. While it exists as a gas above the water dew point, HCl dissolves in condensed water below that point, forming acidic solutions that initiate corrosion [2, 8]. Temperature, pH, and corrosive species such as H_2S, naphthenic acids, and ammonium salts influence corrosion rates. In particular, proximity to the water dew point intensifies corrosion, with pH playing a central role in corrosion severity [2, 8, 9].

Chemical treatment remains one of the most effective mitigation strategies in refineries [4, 10]. Sodium hydroxide (NaOH) is injected into the crude feed to neutralize hydrolyzable salts such as $MgCl_2$ and $CaCl_2$ and prevent HCl formation [5, 11]. Additional treatments, including ammonia, organic amines and corrosion inhibitors, further stabilize the system by neutralizing acidic condensates [12, 13]. Effective corrosion management depends on strong monitoring systems [14]. Measurements of pH, chloride, and dissolved iron in overhead water provide critical data for optimizing chemical dosing strategies [2, 7, 15-17].

Despite the widespread application of chemical treatment and monitoring, understanding how these parameters interact under actual operating conditions remains limited. Most studies focus on isolated variables or controlled laboratory setups, leaving a gap in field-based evidence that links water chemistry to corrosion behavior. This study addresses that gap by integrating condensate analysis, corrosion rate measurements, and operational inspections to develop a practical framework for optimizing chemical treatment. The goal is to improve corrosion

control, reduce unplanned downtime, and extend the life of critical distillation infrastructure.

2. Materials and Methods

2.1. Materials

2.1.1. Crude Oil

The main feedstock for the atmospheric distillation units of the Thi-Qar Refinery was crude oil that was obtained from the Rumaila oil fields for this study. The crude oil has the following physical and chemical characteristics: density 0.8854 g/cm³, viscosity 11.7 cSt, water/sediment 0.3 vol%, salt 136 ppm, sulphur 3.345 wt%, and API 28.2.

2.1.2. Caustic Soda (NaOH)

25-kg packages of white solid flakes with 95% purity were used to keep salts stable. It has the following characteristics: MW 39.998 g/mol, melting point 318 °C, and water solubility.

2.1.3. Neutralizing Amine

In this investigation, Petromeen, a commercial neutralising amine produced by Veolia (UAE origin), was used. Its chemical makeup includes monoethanolamine (MEA), which the crude distillation unit uses as a pH neutraliser. MEA's physicochemical characteristics include its ammonia-like odour, density of 1.017 g/cm³, pH of 11.2 (1%), and a boiling range of 70–172 °C.

2.1.4. Film-Forming Corrosion Inhibitor

Veolia (UAE-based) provides Philmplus 5065D, a commercial film-forming corrosion inhibitor. This inhibitor's physicochemical properties include a density of 7.5 lbs/gal, a viscosity of 9 mPa·s, a pH of 6.3 (1%), and an insoluble nature in water.

2.2. Analytical Methods

2.2.1. Water Chemistry Analysis

The overhead condensed water was analyzed for its key chemical properties using the following methods:

- **pH Measurement**: The pH was measured using a WTW inoLab® pH 7110 device (UK origin). The electrode was immersed directly into a freshly collected overhead condensate sample, and the pH reading was recorded digitally.
- **Chloride Ion Concentration**: Chloride levels in the overhead water samples were determined using the standard titration method, in accordance with ASTM D512-12 [18].

- **Iron Ion Concentration**: A HACH DR3900 UV-Vis spectrophotometer (Germany) was used to measure the concentration of dissolved iron. The instrument employed the FerroVer® Iron Method 265, along with pre-programmed protocols tailored to reagent-specific reactions.

To ensure data reliability, all pH and Fe^{2+} measurements were repeated in triplicate, and the results were reported as mean values with corresponding standard deviations.

2.2.2. Chemical Solution Analysis

The caustic solution prepared for injection into the crude feed line was analyzed using acid-base titration to accurately determine its concentration prior to field application.

2.2.3. Rate of Corrosion Measurements

To simulate the corrosive environment found at the top of an atmospheric distillation column, we conducted a laboratory test using real condensed water from an operating refinery and standard carbon steel samples known as corrosion coupons.

These steel samples were made from ASTM A283 Grade C carbon steel, commonly used in refinery equipment [19]. Each coupon measured 100 mm × 100 mm × 6 mm, as shown in Fig. 1. The condensed water was collected under stable operating conditions, then sealed immediately to avoid contamination and stored at 60 °C until use.

Before testing, the steel test pieces were prepared with dimensions of 100 × 100 × 6 mm and mechanically polished with silicon carbide paper grades 400–1200 to clean the surface. They were then cleaned with ethanol and left to dry in the air. We confirmed the metal composition using a technique called optical emission spectroscopy, ensuring it matched the steel used in refinery piping and components (see Table 1).

Although the lab setup couldn't fully mimic the flow and pressure conditions inside a real distillation column, it closely replicated key chemical properties—like pH, ion concentrations, and dissolved gases. Because of this, the corrosion results were used to observe general trends, not exact corrosion rates.

To ensure reliability, each test was repeated with at least three steel coupons. The corrosion was measured by how much weight each sample lost during exposure. These values were reported as averages, along with standard deviations, to show the consistency of the results.

Fig. (1): Standard carbon steel coupons (ASTM A283-Gr.C).

Table (1): The chemical composition of carbon steel coupons (ASTM A283-Gr.C).

Elements	Carbon	Manganese	Phosphorous	Sulfur	Silicon	Copper
Samples	0.19	0.19	0.022	0.014	0.36	0.27
A283-Gr.C	0.24 Max.	0.90 Max.	0.035 Max	0.040 Max.	0.40 Max.	0.20 Min.

3. Results and Discussion

3.1. Factors affecting the overhead system's corrosion

With an emphasis on crude oil chemistry, chemical additive performance, and corrosion rate measurements, this research offers an experimental evaluation of the variables affecting corrosion in the overhead system of atmospheric distillation columns. Clarifying corrosion severity under various operating settings and assessing chemical mitigation techniques are the goals. The behavior of corrosion in overhead systems is largely determined by the chemical makeup of crude oil. Sulphur concentration, total salt content, and bottom sediment and water (BS&W) are important factors [20]. Early 2024 data, as shown in Figure (2), revealed BS&W levels ranging from 0.1 to 0.4 vol.%, which is higher than the generally recognised 0.1 vol.% corrosivity threshold. Through H_2S or CO_2 interactions, high BS&W encourages the development of acidic condensate, escalating localised corrosion processes such as pitting and crevice corrosion. The corrosive threshold of 10 ppm was greatly exceeded by the salt levels, which varied from 136 to 260 ppm.

Pitting and stress corrosion cracking result from the hydrolysis of elevated magnesium and calcium chloride levels under heat, which produces HCl [21]. The creation of H_2S, which dissolves in water to produce corrosive acids that cause sulphide stress cracking and hydrogen embrittlement, was made possible by the sulphur content reaching 3.35 wt.%, which was far higher than the crucial limit of 0.1 wt.%. Although temperatures above 200°C are often linked

to naphthenic acid corrosion, the lower temperatures of the overhead system suggest that wet H_2S is the primary corrosion driver [22, 23].

Chemical treatments were applied by injecting caustic into the crude input line, while neutraliser and filming amines were introduced into the overhead line after being diluted with water and light naphtha, respectively. This process optimises pH control and produces protective inhibitor coatings. Depending on the availability of the chemical, four injection regimes (0.5, 1.0, 1.5, and 2.0 L/day) were evaluated. By increasing the alkalinity of the system and neutralising acidic species such as HCl, H_2S, and naphthenic acids, caustic injection decreased acid-driven corrosion. Filming inhibitors and neutralising amines operated together to buffer pH within slightly alkaline limits. According to experimental data, increasing the amine dose from 1 to 2 L/day resulted in a 30% reduction in corrosion-related maintenance, highlighting the need for careful pH control.

Particularly in water-based conditions, chloride ions play a key role in the onset of corrosion. Caustic precipitated insoluble salts, whereas neutralising amines complexed chloride ions, lowering their corrosiveness. Metal surfaces were further protected with film-forming amines (corrosion inhibitors). Laboratory testing indicated that at low salt levels (~60 ppm), caustic (3.5 wt.%) and amine (1 L/day) dosage stabilised pH at ~5.7 and lowered chloride to ~13 ppm, resulting in minimal corrosion rates. Due to increasing salt hydrolysis, the same dosage resulted in higher chloride levels and lower pH at moderate salt levels (~100 ppm) (Standard deviation for pH: ±0.15; for chloride: ±1.1 ppm). Additionally, high Fe^{2+} (>30 ppm) indicated active corrosion. The pH and chloride were brought back to acceptable values by adjusting the caustic to 4.4 wt.% and the amine to 2 litres each day. However, too much caustic (>6 wt.%) raised the pH above 6.5, increasing the risk of fouling, caustic precipitation, and long-term stress corrosion cracking.

The use of chemicals was insufficient under high-salinity conditions (170–200 ppm) because prolonged salt hydrolysis caused low pH and high chloride, highlighting the necessity of upstream desalting to properly prevent corrosion, as shown in Table (2).

Condensed overhead water's iron ion (Fe^{2+}) concentrations provide a sensitive indicator of active corrosion. Increased anodic dissolution as a result of chloride-induced passive layer disintegration and acidic condensate production was reflected in elevated Fe^{2+}, especially in high salinity and water conditions. Protective iron hydroxide layers were precipitated by caustic reaction with Fe^{2+} and Fe^{3+}, and the presence of CO_2 encouraged the production of $FeCO_3$, both of which helped to reduce corrosion. In addition, neutralising amines increased pH, promoted

iron precipitation and complexation, and decreased dissolved iron concentrations, all of which decreased corrosion rates (Mean Fe^{2+}: 0.57 ppm; Standard Deviation: ±0.09 ppm).

Table (2): Laboratory results of crude oil and condensed water from the overhead distillation tower of the third unit in the Thi-Qar refinery.

Date	BS& W% (ppm)	Salt content (ppm)	Sulphur content (wt.%)	pH	Fe^{2+} (mg/L)	Cl^- (mg/L)	NaOH (wt.%)
02/01/2024	0.4	257	3.38	5.1	84.5	5.31	2.6
03/01/2024	1.1	536	3.21	4.9	26.6	10.63	3.4
04/01/2024	0.5	174	3.296	4.8	64.4	10.63	3.2
07/01/2024	0.3	85	3.42	5.1	42.4	19.49	3.5
08/01/2024	0.3	125	3.36	5	40.6	21.27	3.9
10/01/2024	0.3	60	3.4	5.7	76.9	13.04	3.5
11/01/2024	0.2	44	3.44	5.3	14.6	8.8	4.4
14/01/2024	0.2	193	3.4	6.4	51	15.95	4.1
24/01/2024	0.1	100	3.38	5.4	82.1	24.27	3.8
26/01/2024	0.2	148	3.35	5.2	74.6	19.49	5.2
30/01/2024	0.2	94	3.418	5.1	47	15.9	4.4
01/02/2024	0.05	91	3.47	5	85.5	28.36	5
11/02/2024	0.3	64	3.38	4.9	90	17	4.8
20/02/2024	0.4	114	3.353	5.1	62	21	5.6
29/02/2024	0.1	49	3.422	4.6	26	14	4.6
10/03/2024	0.3	136	3.34	4.8	32	14	5.8
20/03/2024	0.2	93	3.32	4.9	65	16	4.9
31/03/2024	0.5	311	3.46	5.4	103	27	4.9
08/04/2024	0.2	61	3.6	4.8	151	28	4.8
21/04/2024	0.3	117	3.36	5.2	86	19	4.8
30/04/2024	0.3	91	3.38	4.7	144	19.4	5.4
12/05/2024	0.3	131	3.5	4.8	122	28	5.9
20/05/2024	0.5	260	3.56	4.7	100	24	4.1
30/05/2024	0.4	160	3.54	3.9	90	14	4
10/06/2024	0.2	105	3.47	5.1	87	14	3.5

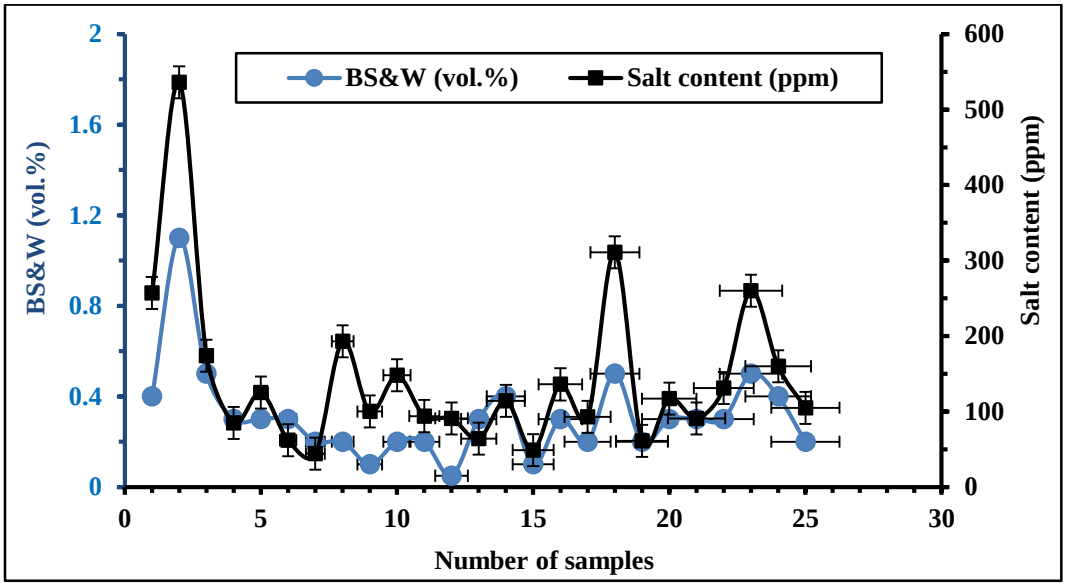

Fig. (2): Variation in BS&W content (vol%) and salt concentration (ppm) in crude oil samples from Jan–Jun 2024. Error bars represent the standard deviation from three replicate measurements.

3.2. Determining the Corrosion Rate Using the Weight Loss Method

Using the weight loss method, the corrosion rate of carbon steel exposed to overhead condensed water was measured as a function of pH in the presence of chemical additives. This method was selected because it quantifies mass loss directly, detects both localised and general corrosion, and suits long exposure times. Condensate samples were subjected to several pH adjustments in order to replicate various corrosive environments. Coupons of carbon steel were first submerged in condensate at pH 4 for 30 days. The specimens were visually examined and verified to be free of contamination or debris before being submerged. After exposure, the final weight was 410.5 g, which represents a 500 mg weight drop from the original coupon weight of 411.0 g. The mean weight loss: 500 mg; Standard Deviation: ±17.6 mg from 3 samples.

The corrosion rate was calculated using Eq. (1) [24]:

$$Corrosion\ Rate\ (mpy) = \frac{22.3 \times Weight\ Loss\ (mg)}{Density\ (g/cm^3) \times Area\ Exposed\ (cm^2) \times Exposure\ Time\ (days)} \ldots\ldots\ldots(1)$$

where “mpy” denotes mils per year (1 mil = 0.001 inch).

The calculated corrosion rate was 7 mpy using an exposed surface area of 88.32 cm² and a density of 7.7 g/cm³ for carbon steel. The value was higher than the 3 mpy maximum level that is approved by the industry [24]. After 30 days, the condensate showed dark brown discoloration indicated the presence of soluble and precipitated corrosion products, including iron oxides, hydroxides, and chlorides. Visual examination confirmed acid-induced attack,

showing both localised and general pitting corrosion on the coupon surface, as shown in Figure (3).

The corrosion rate values of the corrosion rate clearly depended on pH. The corrosion rate was 8.27 mpy at pH 3.5, which is about four times greater than the 1.97 mpy at pH 6.0 as shown in Figure (4) (Error bars added to Figure (4) represent ± 0.3 mpy based on triplicate experiments). This pattern demonstrates how much acidity affects the rate of corrosion. Particularly in situations containing chlorides, increased hydrogen ion concentrations at lower pH enhance localised corrosion by promoting electrochemical processes such as hydrogen ion reduction. Acidic environments can cause protective films like FeS or FeO_4 to develop; these layers are frequently unstable and have little corrosion resistance.

The lowest corrosion rates were observed between pH 5.5 and 6.5, with measured values below 1.98 mpy, indicating minimal corrosion risk. The development of more stable passive films, such as $Fe(OH)_3$ or $FeCO_3$, which prevent corrosion by lowering electrochemical activity, is responsible for this decrease. The inhibition of cathodic reactions further lowers corrosion rates at higher (alkaline) pH levels. Therefore, it is crucial to maintain an ideal pH between 5.5 and 6.5 in order to reduce corrosion in overhead systems, provide efficient chemical management, and maintain the integrity of equipment. These results are consistent with research showing that mildly acidic environments encourage the production of passive films, lowering the danger of under-deposit corrosion [25, 26].

To track corrosion behavior, dissolved iron concentrations in the overhead condensate were monitored (Table 2). Dissolved iron serves as an indicator of active corrosion or degradation of iron-based components. The measured average iron concentration in acidic condensate was 0.5 ppm ± 0.08, consistent with early-warning thresholds in refinery systems. Exceeding 1 ppm typically signals active degradation requiring intervention. The presence of dissolved iron may also result from the dissolution of protective films such as FeS, Fe_3O_4, $Fe(OH)_3$, and $FeCO_3$, which can deteriorate over time due to prolonged water contact.

Following the 30-day immersion, the corrosion coupon exhibited pronounced morphological degradation (Figure 3). Both generalized and pitting corrosion were observed, consistent with the enrichment of the condensate in dissolved and precipitated corrosion products, primarily iron oxides, hydroxides, and chlorides. The measured corrosion rates, ranging from 1.2 to 4.6 mpy (± 0.35 mpy) under varying salt contents, align with previously reported values. For example, Jasim (2019) reported corrosion rates of approximately 1.5–5 mpy in carbon steel pipelines exposed to CO_2/H_2S-containing crude under comparable temperature and flow

conditions [26]. Kermani and Morshed (2003) summarized field data showing corrosion rates between 1–6 mpy in upstream production systems with CO_2 and salt deposition [12].

To further quantify the observed dependence of corrosion rate on pH, a nonlinear regression analysis was performed using a second-order polynomial model. The resulting correlation, shown in Fig. 4, fits the data with high accuracy ($R^2 = 0.979$), highlighting the strong inverse relationship between corrosion rate and pH in acidic to near-neutral conditions. The best-fit equation, corrosion rate = $1.0607pH^2 - 13.095pH + 42.999$, confirms the trend observed visually, with the minimum corrosion rates occurring between pH 5.5 and 6.5. This quantitative analysis reinforces that maintaining the condensate pH within this optimal range effectively minimizes corrosion risks in overhead systems.

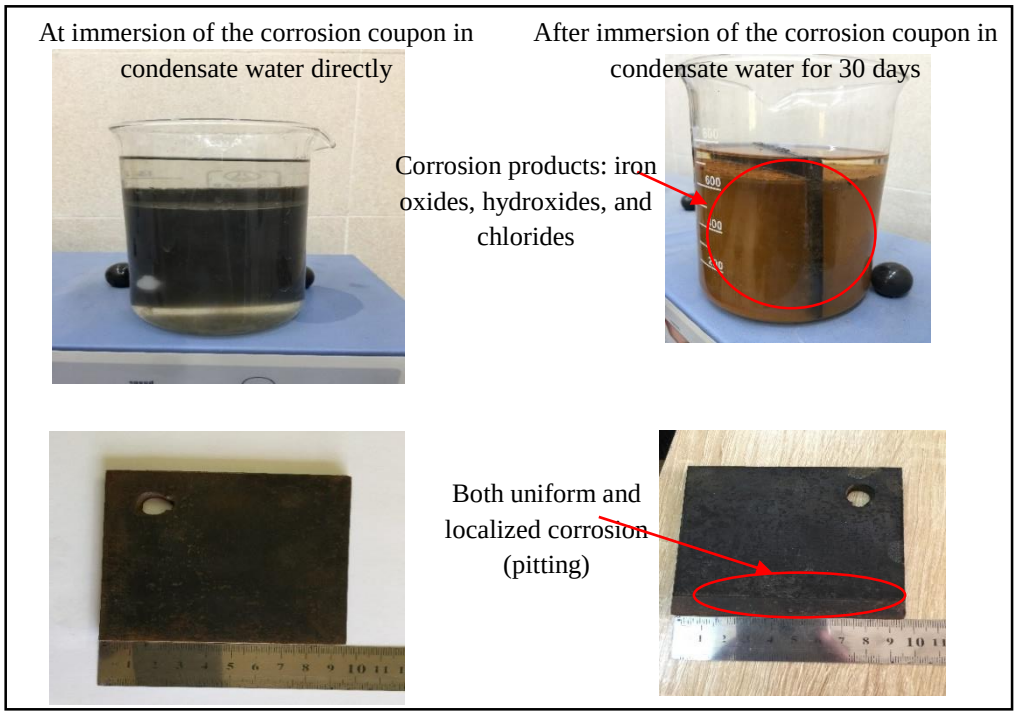

Fig. (3): Corrosion coupon before and after 30-day immersion at 60 °C.

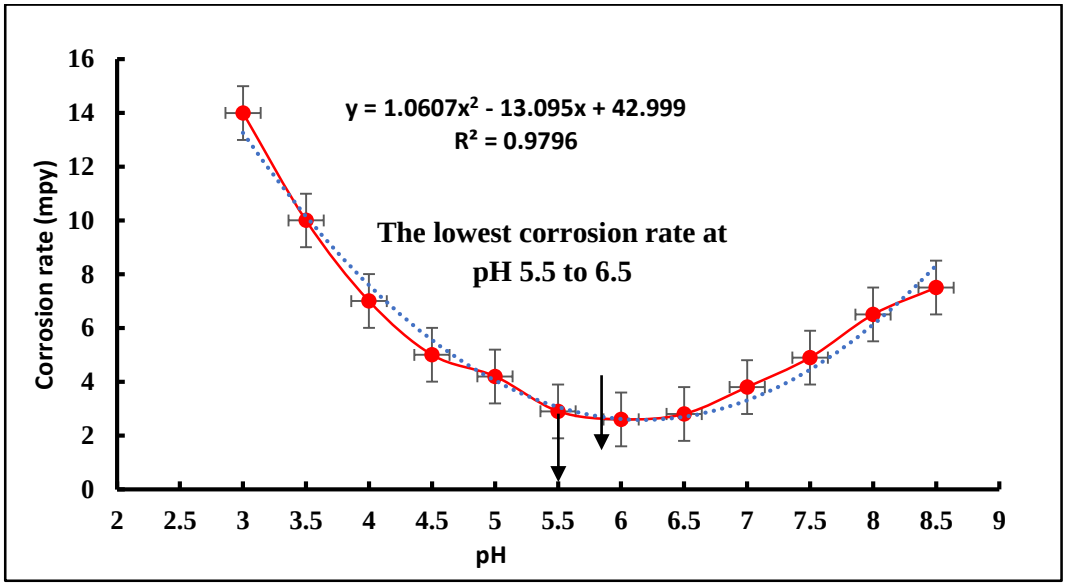

Fig. (4): Effect of pH of condensed water on the corrosion rate.

3.3. Visual Assessment and Corrosion Morphology in the Atmospheric Overhead System

A comprehensive on-site inspection was conducted on the atmospheric distillation column at the Thi-Qar refinery during the 2024 scheduled turnaround, aiming to assess corrosion-related degradation in overhead system components. The column contains 29 trays (numbered 1–29, bottom to top) and is constructed from Monel (Alloy 400, above tray 25), carbon steel (trays 5–25), and martensitic stainless steel (SS410, below tray 5).

Corrosion features were observed across multiple components, including trays, tray supports, column walls, elbows, and condenser tubes. The primary cause was linked to high water and salt content in the crude feed, which exceeded design tolerances throughout early 2024. Notably, a peak salt content of 536 ppm was recorded in January, significantly contributing to the formation of hydrochloric acid (HCl) and ammonium chloride (NH_4Cl) in the overhead system [17]. These compounds are known to induce aggressive localized corrosion, particularly under subcooled and condensing conditions. Photographic and visual evidence (Figure 5a–5f) revealed the following key damage mechanisms:

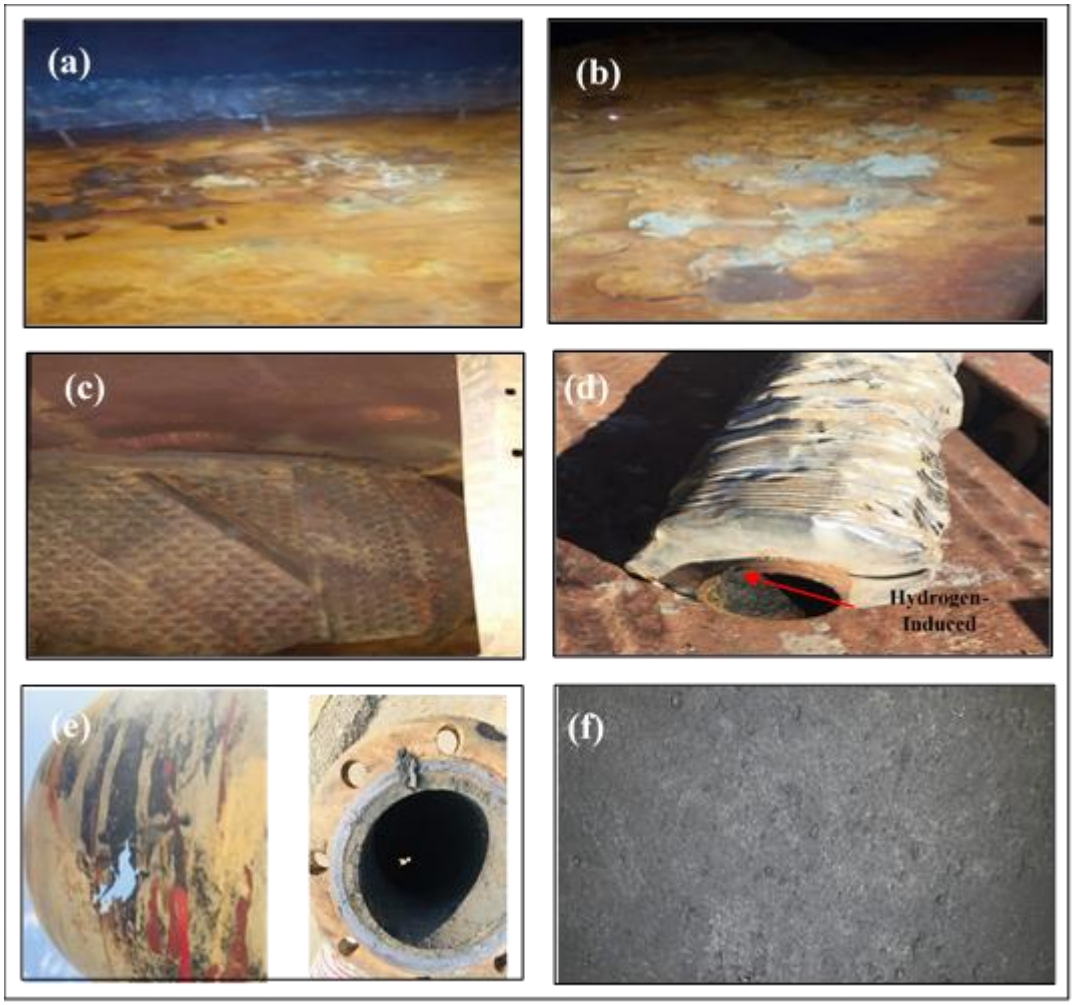

Fig. (5): Images of some areas of the atmospheric overhead system.

The surface of Tray 28 shows advanced general corrosion and through-wall perforation (Figure 5a). Yellow and white salt deposits are visible and are attributed to sulfur and ammonium compounds, respectively. Tray 24 displays extensive corrosion and enlarged orifice openings caused by metal loss (Figure 5b). The valve openings are deformed, indicating potential operational impairment. The tray support structure has collapsed due to corrosion-induced weakening and metal fatigue, as shown in Figure (5c). In the finned tubes of the air-cooled exchanger, hydrogen-induced cracking (HIC) and severe wall thinning were observed (Figure 5d). This damage is consistent with wet H_2S exposure. The external elbow section shows visible coating degradation and under-film corrosion in a high-flow zone (Figure 5e). The internal surface of the manifold elbow shows signs of erosion-corrosion due to entrained solids in the condensate flow. The distillation column wall exhibits localized pitting corrosion attributed to acidic condensate attack (Figure 5f).

Complementary residue analysis [16] of samples from trays 23–29 revealed that the deposit

matrix was predominantly non-volatile at 500 °C, with more than 90% composed of water- and HCl-soluble compounds, further confirming the presence of salts and corrosion products. The findings support the conclusion that HCl and NH_4Cl are dominant contributors to corrosion in the atmospheric overhead system, with secondary effects from wet H_2S and erosive particle-laden flows.

3.4. Corrosion Mechanisms and Causes in the Atmospheric Overhead System

Effective corrosion management in refinery overhead systems requires a clear understanding of the major degradation mechanisms and their interactions [27]. Based on experimental results, coupon inspection, and supporting literature, five dominant corrosion mechanisms were identified, with emphasis on how they correlate and reinforce one another under typical refinery conditions.

To reduce redundancy, overlapping content with the discussion section has been consolidated, and a schematic (Figure 6) has been created to visualize the interaction among the following mechanisms:

3.4.1. Chloride-Induced Corrosion:

Two dominant forms of chloride-induced corrosion were observed:

- Hydrogen chloride (HCl) corrosion: Arises from the hydrolysis of calcium and magnesium chloride during crude preheating. The resulting HCl dissolves in the condensate, generating a low-pH environment that accelerates uniform and pitting corrosion.
- Ammonium chloride (NH_4Cl) corrosion: Forms when HCl reacts with ammonia (generated from nitrogen compounds in crude). NH_4Cl deposits are hygroscopic and support under-deposit corrosion in subcooled areas. Deposits were visually confirmed in the tray and inside finned tube regions (see Figure 5a–5d).

Laboratory tests confirmed that corrosion rates decreased significantly in the pH range of 5.5–6.5. Coupon immersion studies (30 days) showed reduced mass loss and shallow pitting within this range, supporting the pH-sensitive behavior of chloride-based corrosion (see Figure 3).

3.4.2. Wet H_2S Damage:

Wet hydrogen sulfide (H_2S) corrosion is a significant degradation mechanism in overhead systems, particularly in condensers. Visual inspection (Figure 5d) revealed clear signs of hydrogen-induced cracking (HIC) in the finned tubes, confirming the occurrence of wet H_2S damage. This type of corrosion begins when H_2S reacts with iron surfaces to form iron sulfide (FeS), a semiconductive film that

accelerates the dissociation of H_2S and facilitates the entry of atomic hydrogen into the steel matrix. The presence of water enables further reactions where H_2S and oxygenated species generate sulfuric acid sulfuric acid (H_2SO_4), intensifying the acidic environment:

$$H_2S + 4H_2O \rightarrow H_2SO_4 + 4H_2 \quad \text{…….. (2)}$$

$$H_2SO_4 + Fe \rightarrow FeSO_4 + H_2 \quad \text{……(3)}$$

$$H_2S + Fe \rightarrow FeS + H_2 \quad \text{…….(4)}$$

The atomic hydrogen produced in these reactions diffuses into steel, accumulates at internal defects, and recombines to form molecular hydrogen. This creates high local pressures that result in Blistering, Hydrogen-induced cracking (HIC), Stress-oriented hydrogen-induced cracking (SOHIC), and Sulfide stress cracking (SSC). These damage modes reduce mechanical integrity and thermal efficiency, and can lead to unplanned shutdowns. The onset of such corrosion was also supported by elevated Fe^{2+} concentrations in condensate samples and pH reductions under high salt and water loading, indicating active anodic dissolution and film breakdown.

3.4.3. CO_2 Corrosion: Carbon dioxide reacts with water to form carbonic acid, which attacks steel surfaces. At 60–100 °C, CO_2 corrosion contributes to general thinning. In systems where H_2S is also present ($H_2S/CO_2 > 1:200$), FeS forms and may either shield or promote localized damage depending on flow and pH.

3.4.4. Organic Acid Corrosion: Low-molecular-weight organic acids such as formic and acetic acids, along with residual naphthenic acids, attack metal surfaces in stagnant zones [28]. These acids dissolve protective layers and intensify localized corrosion. Though naphthenic acid corrosion is more active above 200 °C, acidic condensate at lower temperatures still promotes localized degradation.

3.4.5. Erosion and Erosion-Corrosion: Fast-moving two-phase flows carrying solids (e.g., iron oxides) produce mechanical damage coupled with chemical attack [29]. Erosion grooves, U-shaped wall loss near bends and valves, and thinning of elbow surfaces were observed (see Figure 5e).

3.4.6. Mechanism Interactions and Mitigation:

These mechanisms frequently act in combination. For example, chloride corrosion promotes Fe^{2+} release, which combines with H_2S or CO_2 to form weak protective films like FeS or $FeCO_3$. Simultaneously, ammonia from nitrogen compounds can lead to NH_4Cl deposition.

Chemical treatments include:

- Caustic Injection: Neutralizes HCl, stabilizes pH

- Neutralizing Amines: Complex chloride ions increase pH
- Filming Amines: Create a physical barrier on metal surfaces

Figure (6), summarizes the interplay between these corrosion mechanisms, showing spatial interaction of major corrosion types (1: Chloride-induced, 2: Wet H_2S, 3: Erosion-corrosion, 4: CO_2, 5: Organic acids). Data supported by experimental results, visual inspection, and literature [12]; [26]; API RP 571 [30].

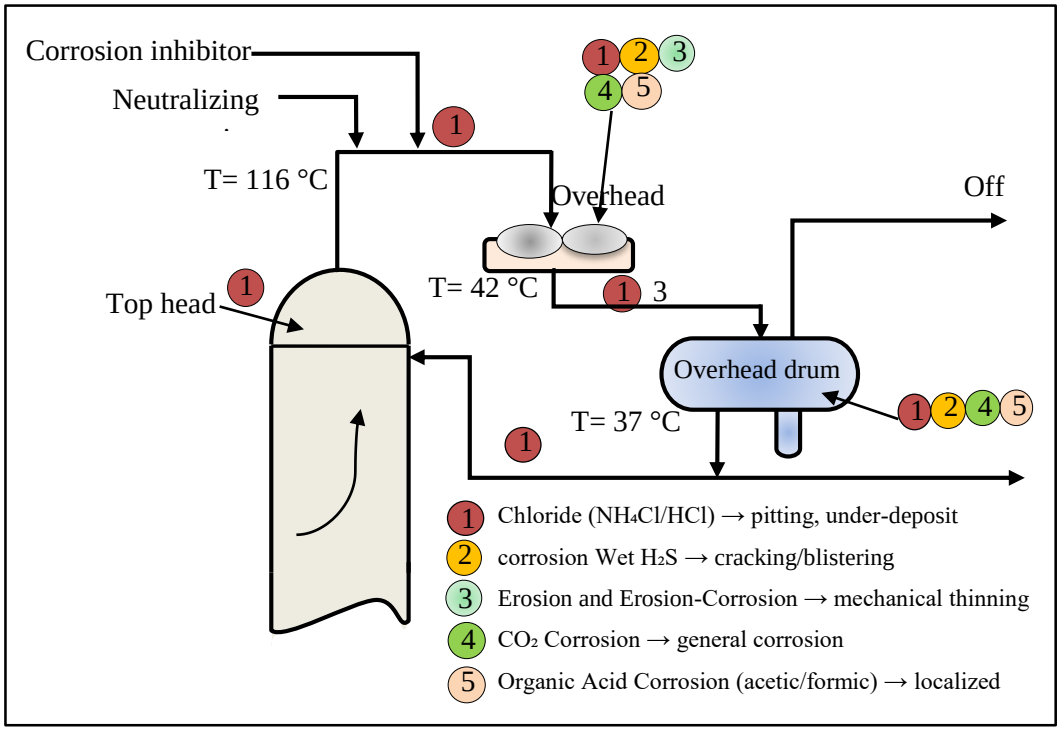

Fig. (6): The corrosion mechanisms in the overhead system in atmospheric distillation units.

4. Conclusions

The study demonstrates that corrosion behavior in the overhead system of distillation columns is strongly associated with the chemical and physical properties of the processed crude oil, particularly bottom sediment and water (BS&W), total salt, and sulfur content. Effective corrosion management requires precise regulation of caustic and neutralizing amine injections to control pH and chloride (Cl^-) concentrations in the overhead condensed water. Elevated iron ion levels in the overhead water serve as reliable indicators of active corrosion and require intensified chemical treatment and enhanced monitoring.

Experimental weight-loss results confirm that corrosion rates are highly pH-dependent, with the lowest rates (~1.9 mpy) observed within the near-neutral range of pH 5.5–6.5. Metallurgical assessments revealed several interacting degradation mechanisms, including chloride-induced

pitting, sulfide stress cracking caused by wet H_2S, erosion-corrosion under high-flow conditions, CO_2-induced acid corrosion, and localized attack by organic acids.

The neutralizing amine reacts with HCl and H_2S, raising the condensate pH, while caustic (NaOH) provides alkalinity to reduce acidic gas solubility. Corrosion inhibitors complement this by forming an adsorbed protective film, minimizing metal interaction with corrosive species like Cl^-, H^+, and S^{2-}.

Experimental data indicate that effective mitigation strategies include maintaining caustic dosages below 5 wt%, neutralizing amine injections between 1–2 L/day, pH within 5.5–6.5, and chloride levels under 20 ppm.

These findings underscore the need for the following actionable steps:

- Implement online pH and Fe^{2+} sensors in overhead water outlets to support real-time corrosion monitoring
- Integrate automated dosing systems to dynamically adjust caustic and amine injection rates based on feedback from live water chemistry data.
- Conduct weekly weight-loss coupon inspections and monthly metallurgical evaluations to detect early degradation trends.
- Establish operational alarm thresholds for pH (<5.5 or >6.5) and Fe^{2+} concentration (>1 ppm) to trigger corrective actions.
- Train operators on interpreting corrosion data and adjusting chemical treatment accordingly to prevent underdosing or overdosing

These recommendations shift corrosion control from a reactive to a predictive and adaptive framework, enhancing operational reliability under variable crude environments.

Author Contributions Statement: Mahmoud Alhreez contributed to the Conception; Methodology; Investigation/ Experiments; Data Analysis and Interpretation; Writing Original Draft; Writing – Review & Editing. Aliaa S. Abd Al-ameer contributed to the Investigation/ Experiments; Writing Original Draft; Writing – Review & Editing. Zolfa Q. Atshan contributed to the Methodology; Simulation; Writing – Review & Editing. Xin Xiao contributed to the Conception; Data Analysis and Interpretation; Writing – Review & Editing. All authors have read and approved the final version of the manuscript.

References

[1] S. N. Shattab, W. S. Khudair, M.A. Mohammed, and M.A. Kahthim, "Corrosion in Crude Oil Distillation Units (CDUs) and a Study of Reducing Its Rates by Changing Chemical Injection Sites", *Journal of Petroleum Research and Studies*, vol. 13, no. 3, pp. 143-161, 2023. https://doi.org/10.52716/jprs.v13i3.718.

[2] K. A. Mohammed, "Corrosion Control Mechanisms and the Effect of pH on Corrosion in the Crude Oil Refining Process", *Journal of Petroleum Research and Studies*, vol. 12, no. 1(Suppl.), pp. 270-289, Apr. 2022. https://doi.org/10.52716/jprs.v12i1(Suppl.).637.

[3] D. E. P. Klenam, F. McBagonluri, O. S. Bamisaye, T. K. Asumadu, N. K. Ankah, M. O. Bodunrin, A. Andrews, and W. O. Soboyejo, "Corrosion resistant materials in high-pressure high-temperature oil wells: An overview and potential application of complex concentrated alloys", *Engineering Failure Analysis*, vol. 157, p. 107920, 2024. https://doi.org/10.1016/j.engfailanal.2023.107920.

[4] P. F. Timmins, "Failure control in process operations", ASM Handbook Committee, vol. 19, pp. 468 - 482, 1996. https://doi.org/10.31399/asm.hb.v19.a0002387.

[5] A. Bagdasarian, J. Feather, B. Hull, R. Stephenson; and R. Strong, "Crude unit corrosion and corrosion control", Proceedings of *the CORROSION 1996*, p. 1-15, 1996. https://doi.org/10.5006/C1996-96615.

[6] M. A. Fajobi, R. T. Loto, and O. O. Oluwole, "Corrosion in crude distillation overhead system: A review", *Journal of Bio-and Tribo-Corrosion*, vol. 5, no. 3, p. 67, 2019. https://doi.org/10.1007/s40735-019-0262-4.

[7] B. Varbai, R. Wéber, B. Farkas, P. Danyi, A. Krójer, R. Locskai, G. Bohács, and C. Hős, "Application of regression models on the prediction of corrosion degradation of a crude oil distillation unit", *Advances in Materials Science*, vol. 24, no. 1, pp. 72-85, 2024. https://doi.org/10.2478/adms-2024-0005.

[8] H. Li, Y. Yoon, and R. D. Kane, "Study of Aqueous Ammonium Chloride Corrosion in Refinery Crude Distillation Unit Overhead Conditions", in *CONFERENCE 2025*, Association for Materials Protection and Performance, 2025. https://doi.org/10.5006/C2025-00232.

[9] J. A. P. Nicacio, F.C. Oliveira, and M.R. Dumont, "Failure analysis and electrochemical testing of ammonium chloride corrosion in a heat exchanger in a diesel hydrotreating unit of a petroleum refinery", *Engineering Failure Analysis*, vol. 156, p. 107758, 2024. https://doi.org/10.1016/j.engfailanal.2023.107758.

[10] M. Alhreez, and D. Wen, "Controlled releases of asphaltene inhibitors by nanoemulsions", *Fuel*, vol. 234, pp. 538-548, 2018. https://doi.org/10.1016/j.fuel.2018.06.079.

[11] A. S. Yaro, H. Al-Jendeel, and A. A. Khadom, "Cathodic protection system of copper–zinc–saline water in presence of bacteria. Desalination", vol. 270, no. 1-3, pp. 193-198, 2011. https://doi.org/10.1016/j.desal.2010.11.045.

[12] M. Kermani, and A. Morshed, "Carbon dioxide corrosion in oil and gas productiona compendium", *Corrosion*, vol. 59, no. 8, pp. 659–683, 2003. https://doi.org/10.5006/1.3277596.

[13] A. H. Al-Moubaraki, and I. B. Obot, "Corrosion challenges in petroleum refinery operations: Sources, mechanisms, mitigation, and future outlook", *Journal of Saudi Chemical Society*, vol. 25, no. 12, p. 101370, 2021. https://doi.org/10.1016/j.jscs.2021.101370.

[14] R. W. Gaikwad, A. R. Warade, S. L. Bhagat, and J. B. Bhasarkar, "Optimization and simulation of refinery vacuum column with an overhead condenser", *Materials Today: Proceedings*, vol. 57, part 4, pp. 1593-1597, 2022. https://doi.org/10.1016/j.matpr.2021.12.175.

[15] T. Chis, A. E. Sterpu, and O. V. Săpunaru, "The Effect of Corrosion on Crude Oil Distillation Plants", *ChemEngineering*, vol. 6, no. 3, p. 41, 2022. https://doi.org/10.3390/chemengineering6030041.

[16] Arjang, S., K. Motahari, and M. Saidi, "Experimental and modeling study of organic chloride compounds removal from naphtha fraction of contaminated crude oil using sintered γ-Al_2O_3 nanoparticles: equilibrium, kinetic, and thermodynamic analysis", *Energy & Fuels*, vol. 32, no. 3, pp. 4025-4039, 2018. https://doi.org/10.1021/acs.energyfuels.7b03845.

[17] L. Zhou, Q. Zhao, G. Lv, Z. Dou, W. Mu, and T. Zhang, "Effect of NH4Cl on the rusting leaching behavior of metallic phase of iron in reduced ilmenite during TiO_2 purification: An electrochemical and density-functional theory study", *Applied Surface Science*, vol. 638, p. 158019, 2023. https://doi.org/10.1016/j.apsusc.2023.158019.

[18] ASTM D512-12, "Standard Test Methods for Chloride Ion In Water", 2012, *ASTM International: West Conshohocken*, PA, USA, 2012. https://doi.org/10.1520/D0512-12.

[19] S. S. Miftin, and M.S. Hwini, "Measurement of Corrosion Rate in Storage Tank of Crude Oil", Journal *of Petroleum Research and Studies*, vol. 14, no. 4, pp. 129-139, Dec. 2024. http://doi.org/10.52716/jprs.v14i4.818.

[20] A. Groysman, "Corrosion problems and solutions in oil refining and petrochemical industry", *Koroze a ochrana materialu*, vol. 61, no. 3, pp. 100-117, 2017. https://doi.org/10.1515/kom-2017-0013.

[21] M. Vakili, P. Koutník, J. Kohout, and Z. Gholami, "Analysis, Assessment, and Mitigation of Stress Corrosion Cracking in Austenitic Stainless Steels in the Oil and Gas Sector: A Review", *Surfaces*, vol. 7, no. 3, pp. 589-642, 2024. https://doi.org/10.3390/surfaces7030040.

[22] M. M. Mapolelo, R. P. Rodgers, G. T. Blakney, A. T. Yen, S. Asomaning, and A. G. Marshall, "Characterization of naphthenic acids in crude oils and naphthenates by electrospray ionization FT-ICR mass spectrometry", *International Journal of Mass Spectrometry*, vol. 300, no. 2-3, pp. 149-157, 2011. https://doi.org/10.1016/j.ijms.2010.06.005.

[23] Y. Yoon, I. Kosacki, and S. Srinivasan, "Naphthenic acid and sulfur containing crude oil corrosion: A comparative review", in *CORROSION 2016*, Association for Materials Protection and Performance, pp. 1-12, 2016. https://doi.org/10.5006/C2016-07598.

[24] C. Subramanian, "Corrosion prevention of crude and vacuum distillation column overheads in a petroleum refinery: A field monitoring study", *Process Safety Progress*, vol. 40, no. 2, p. e12213, 2021. https://doi.org/10.1002/prs.12213.

[25] H. Bai, "Mechanism analysis, anti-corrosion techniques and numerical modeling of corrosion in energy industry", *Oil & Gas Science and Technology–Revue d'IFP Energies nouvelles*, vol. 75, p. 42, 2020. https://doi.org/10.2516/ogst/2020031.

[26] H. H. Jasim, "Evaluation the effect of velocity and temperature on the corrosion rate of crude oil pipeline in the presence of CO2/H2S dissolved gases", *Iraqi Journal of Chemical and Petroleum Engineering*, vol. 20, no. 2, p. 41-50, 2019. https://doi.org/10.31699/IJCPE.2019.2.6.

[27] W. Giesbrecht, G.G. Duggan, and D. Jackson, "Effective Corrosion Control Techniques for Crude Unit Overheads", in the *CORROSION 2002*, p. NACE-02477, Denver, Colorado, April 2002.

[28] J. G. Speight, "High acid crudes", *Gulf Professional Publishing*, 2014.

[29] P. W. Cleary, M. Prakash, J. Ha, N. Stokes, and C. Scott, "Smooth particle hydrodynamics: status and future potential", *Progress in Computational Fluid Dynamics, an International Journal*, vol. 7, no. 2-4, pp. 70-90, 2007. https://doi.org/10.1504/PCFD.2007.013000.

[30] D. Hadzihafizovic, "Damage Mechanisms Affecting Fixed Equipment in the Refining Industry", *Available at SSRN 4781875*, 2023. https://ssrn.com/abstract=4781875.